Supplemtary materials

Climate-driven carbon exchange in German forests before, during and after the 2018 drought: implications of climate forcing uncertainty

H. Moutahir[1,2], H. Imhof[1], P. Labenski[1], E. Haas[1], D. Kraus[1], S. Walther[3], M. Bell[4], C. Markwitz[5] R. Kiese[1], and R. Grote[1]

[1] Institute of Meteorology and Climate Research Atmospheric Environmental Research (IMK-IFU), Karlsruhe Institute of Technology (KIT), Garmisch-Partenkirchen, Germany
[2] Faculty of Environment and Natural Resources, Albert-Ludwigs-University Freiburg, Freiburg, Germany
[3] Max Planck Institute for Biogeochemistry, Jena, Germany
[4] Forest Research, Alice Holt Lodge, Farnham, Surrey GU10 4LH, UK
[5] University of Göttingen – Bioclimatology, Büsgenweg 2, 37077 Göttingen, Germany

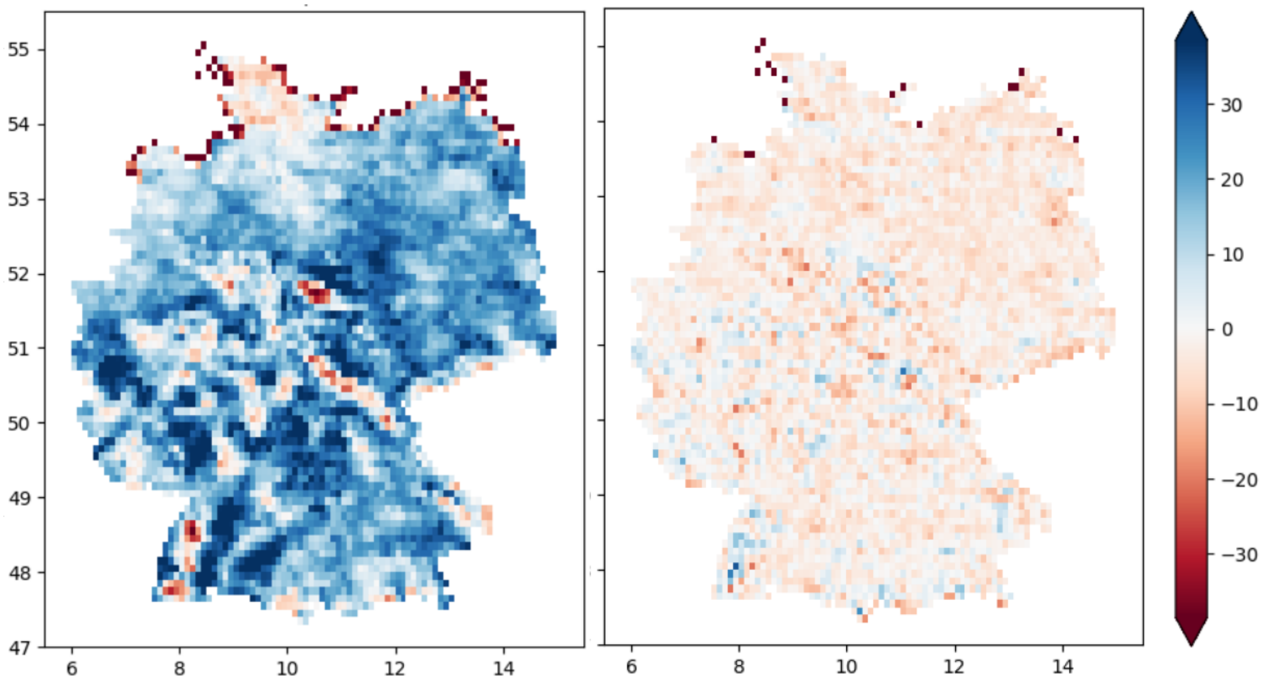

Fig. S1: Relative difference (%) between gridded climate datasets and the German Weather Service (DWD) precipitation observations averaged over 2011–2023. E-OBS closely reproduces observed precipitation patterns (<3% on average), whereas ERA5-Land exhibits a systematic positive bias over large parts of Germany (~20% on average).

Site-level model parameterization and calibration

we selected 3 forest sites in Europe for each of the main tree species which provided data of latent heat flux and net carbon ecosystem exchange for more than 10 years, covering the period from 2011 to 2023. The freely available ICOS data include sites dominated by pine (Brasschaat, Hyytiälä, Loobos), spruce (Tharandt, Davos, BilyKriz) and oak (Hohes Holz, Fontainbleau). The sites have individual labels and key publications in which specific descriptions can be found (BE-bra: Carrara et al. 2003; FI-hyy: Vesala et al. 1998; NL-loo: Bequet et al. 2012; DE-tha: Grünwald & Bernhofer 2007; CH-dav: Etzold et al. 2011; CZ-bil: Sedlak et al. 2013; DE-hoh: Lange et al. 2017; FR-fon: Delpierre et al. 2016). In addition, another oak dominated site from the UK (Straits, Wilkinson et al. 2012) was used, where also long-term eddy-covariance measurements were available. We did the same for beech (Leinefelde in Germany, Soroe in Denmark, and Stitna in the Czech Republic), which was published before in a separate study (Moutahir et al. 2026). Basic site information are given in Table S1 below.

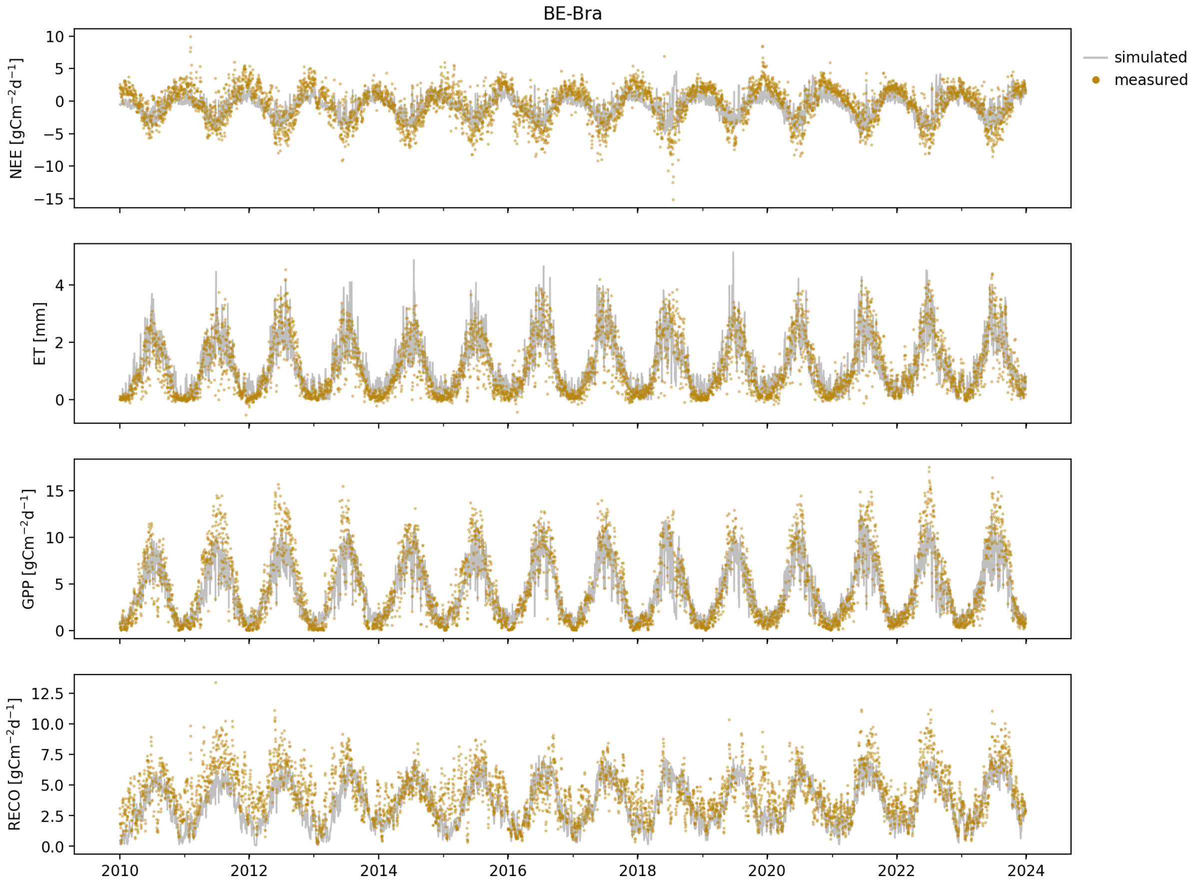
BE-Bra
simulated
measured
NEE [gCm^{-2}d^{-1}]
ET [mm]
GPP [gCm^{-2}d^{-1}]
RECO [gCm^{-2}d^{-1}]
2010
2012
2014
2016
2018
2020
2022
2024

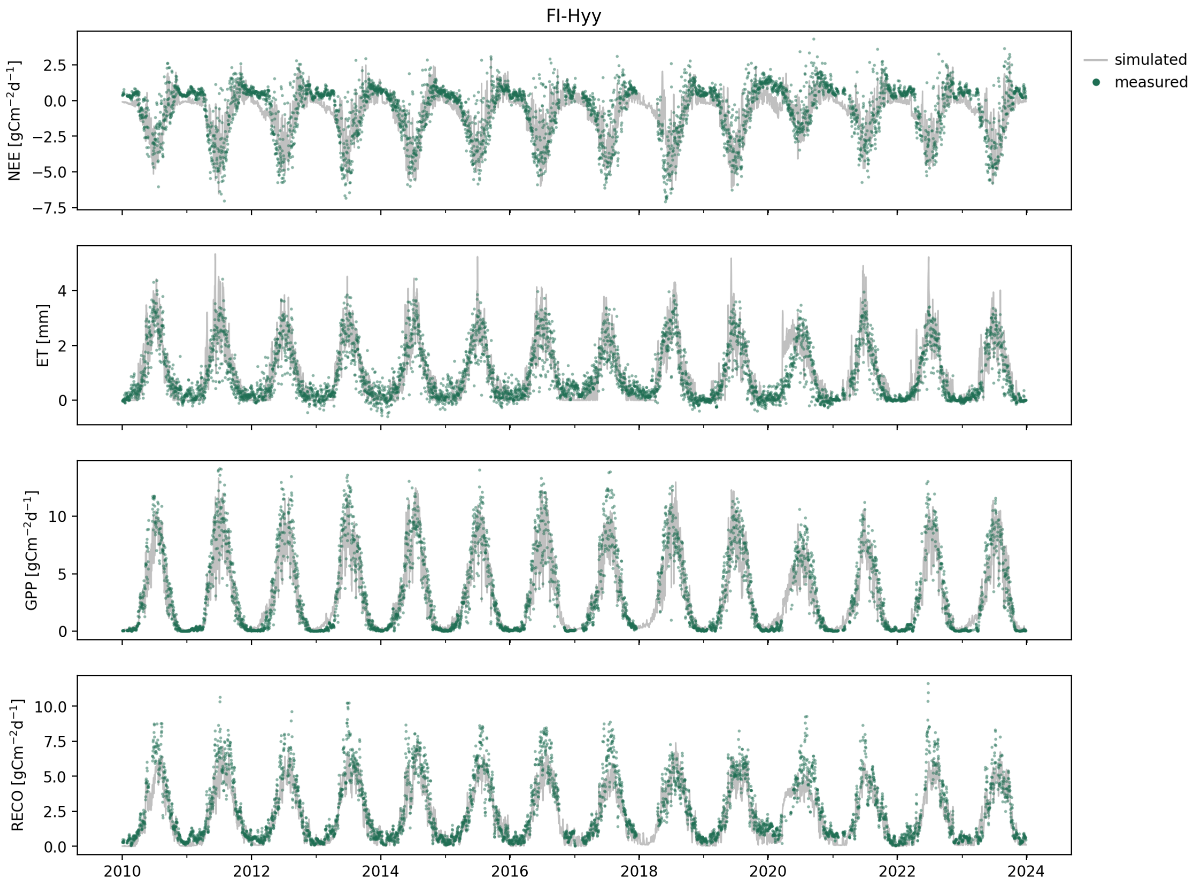
FI-Hyy
simulated
measured
NEE [gCm^{-2}d^{-1}]
ET [mm]
GPP [gCm^{-2}d^{-1}]
RECO [gCm^{-2}d^{-1}]
2010
2012
2014
2016
2018
2020
2022
2024

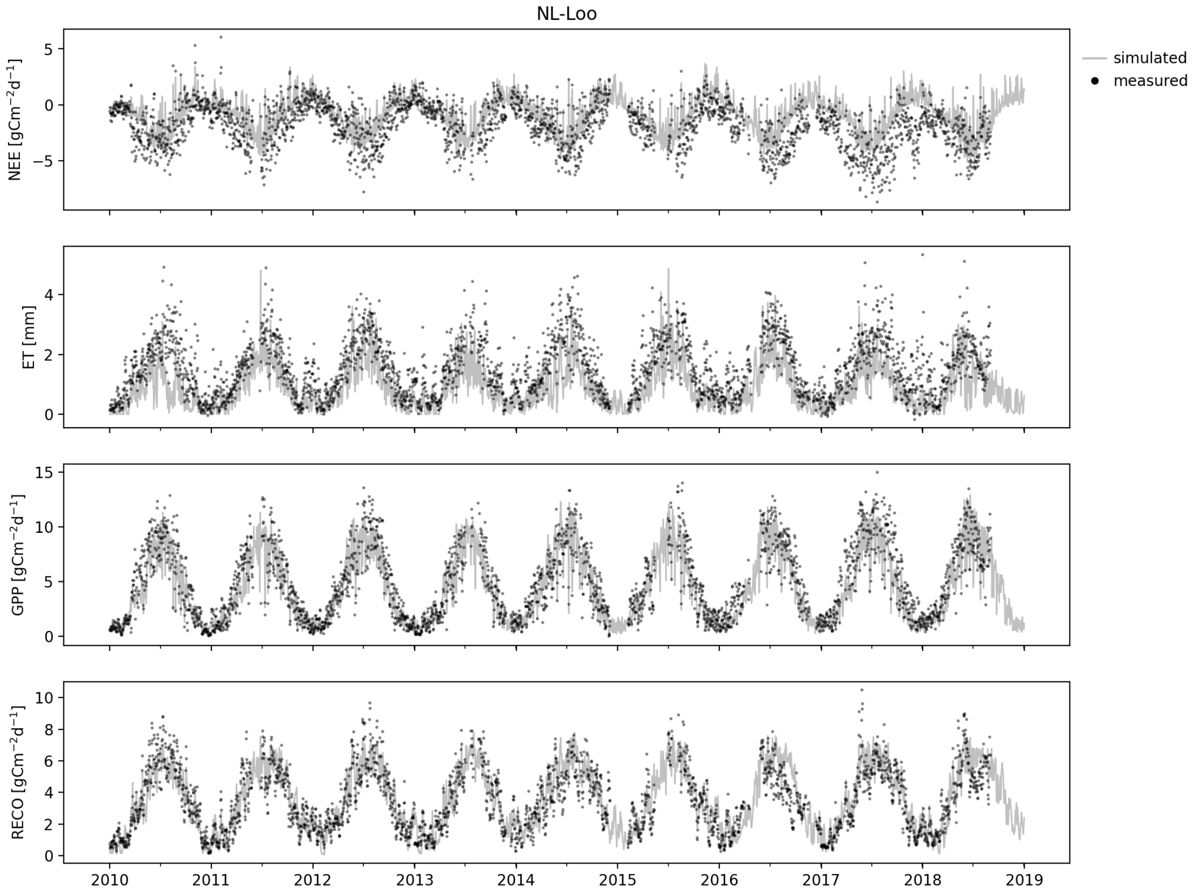

Fig. S2: Comparison of simulated (lines) and measured (dots) daily ecosystem fluxes at three pine sites (top: Brasschaat, BE, black dots; middle: Hyytiälä, FI, yellow dots; bottom: Loobos, NL, green dots) throughout the years 2010-2023. NEE: net carbon exchange (gC m^{-2} d^{-1}), ET: evapotranspiration (mm), GPP: gross primary Productivity (gC m^{-2} d^{-1}), RECO: Ecosystem Respiration (gC m^{-2} d^{-1}).

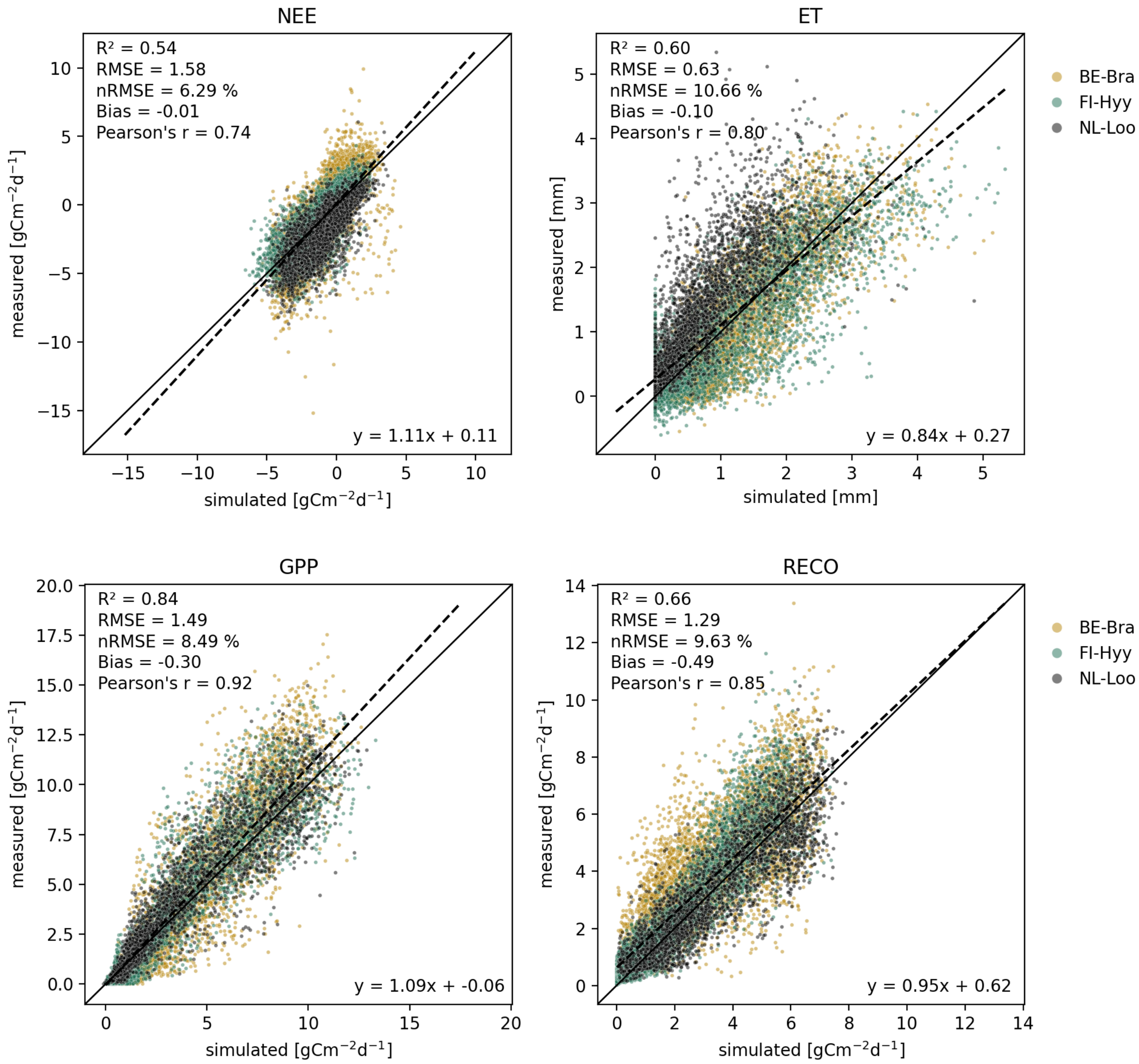

Fig. S3: Evaluation of simulated with measured daily ecosystem fluxes for all three pine sites (see Fig. S1) for the whole available period. NEE (top-left): net ecosystem carbon exchange (gC m^{-2} d^{-1}), ET (top-right): evapotranspiration (mm), GPP (bottom-left): gross primary Productivity (gC m^{-2} d^{-1}), RECO (bottom-right): Ecosystem Respiration (gC m^{-2} d^{-1}). Different sites are depicted in different colors with the same color code as in Figures S1. Metrics include squared coefficient of determination (R^2), relative squared mean error (RSME), normalized relative squared mean error (nRSME), model bias (gC m^{-2} d^{-1} and mm, respectively), and Pearson's coefficient of determination (r).

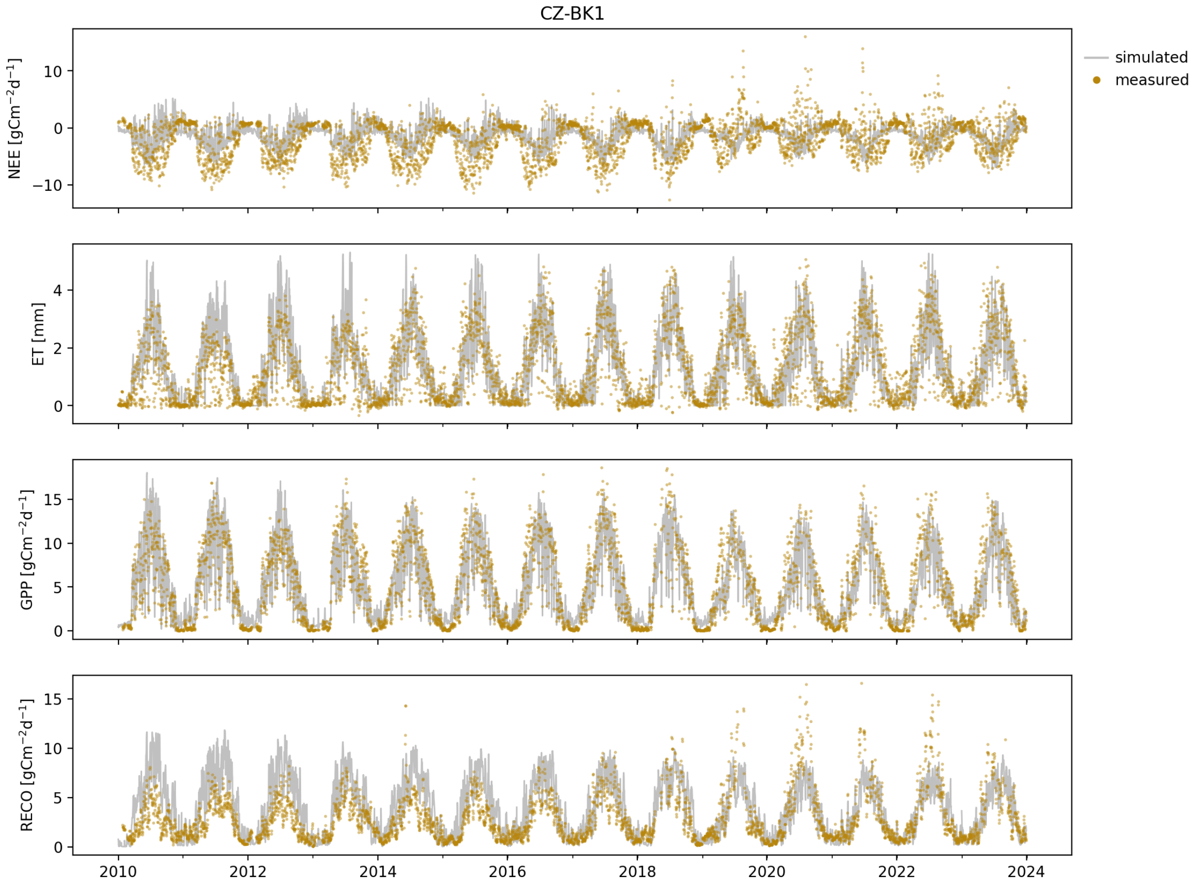

CZ-BK1
NEE [gCm⁻²d⁻¹]
ET [mm]
GPP [gCm⁻²d⁻¹]
RECO [gCm⁻²d⁻¹]
simulated
measured
2010
2012
2014
2016
2018
2020
2022
2024

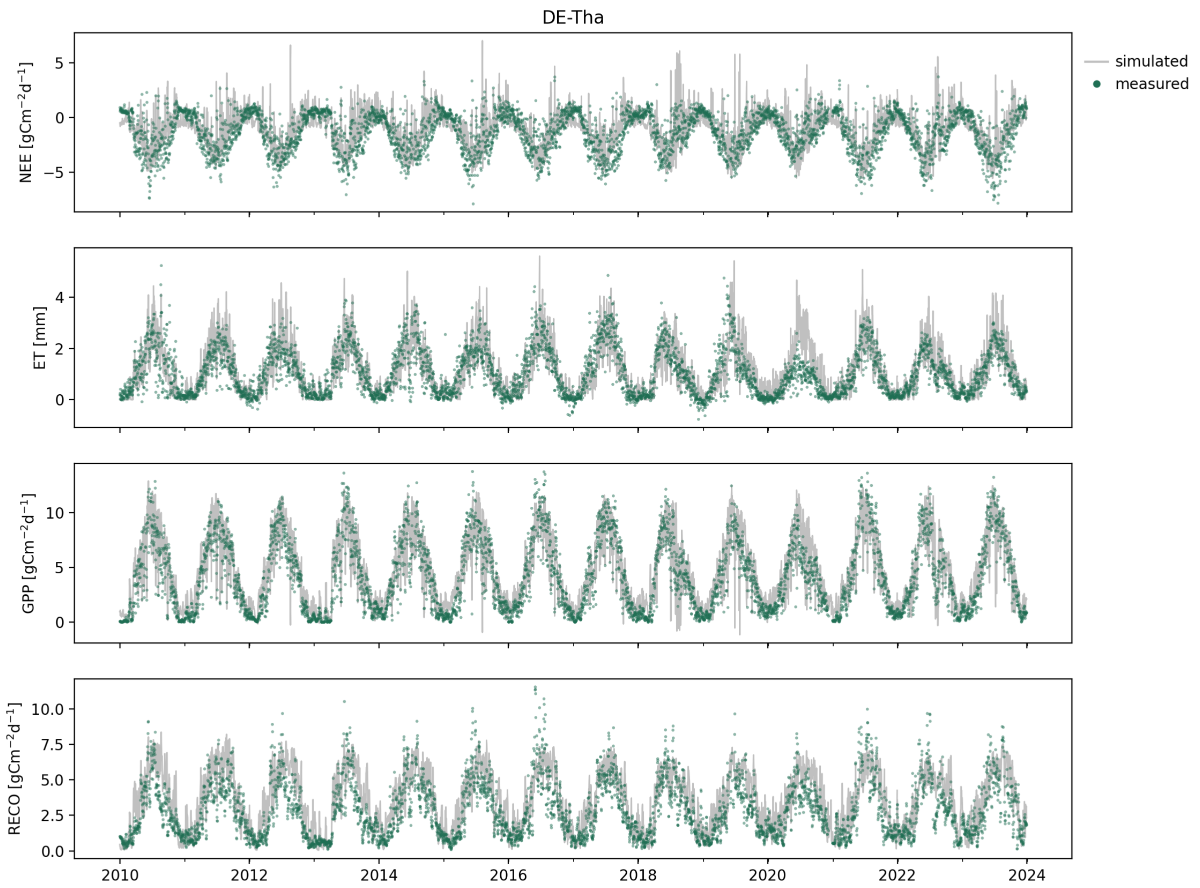

DE-Tha
NEE [gCm⁻²d⁻¹]
ET [mm]
GPP [gCm⁻²d⁻¹]
RECO [gCm⁻²d⁻¹]
simulated
measured
2010
2012
2014
2016
2018
2020
2022
2024

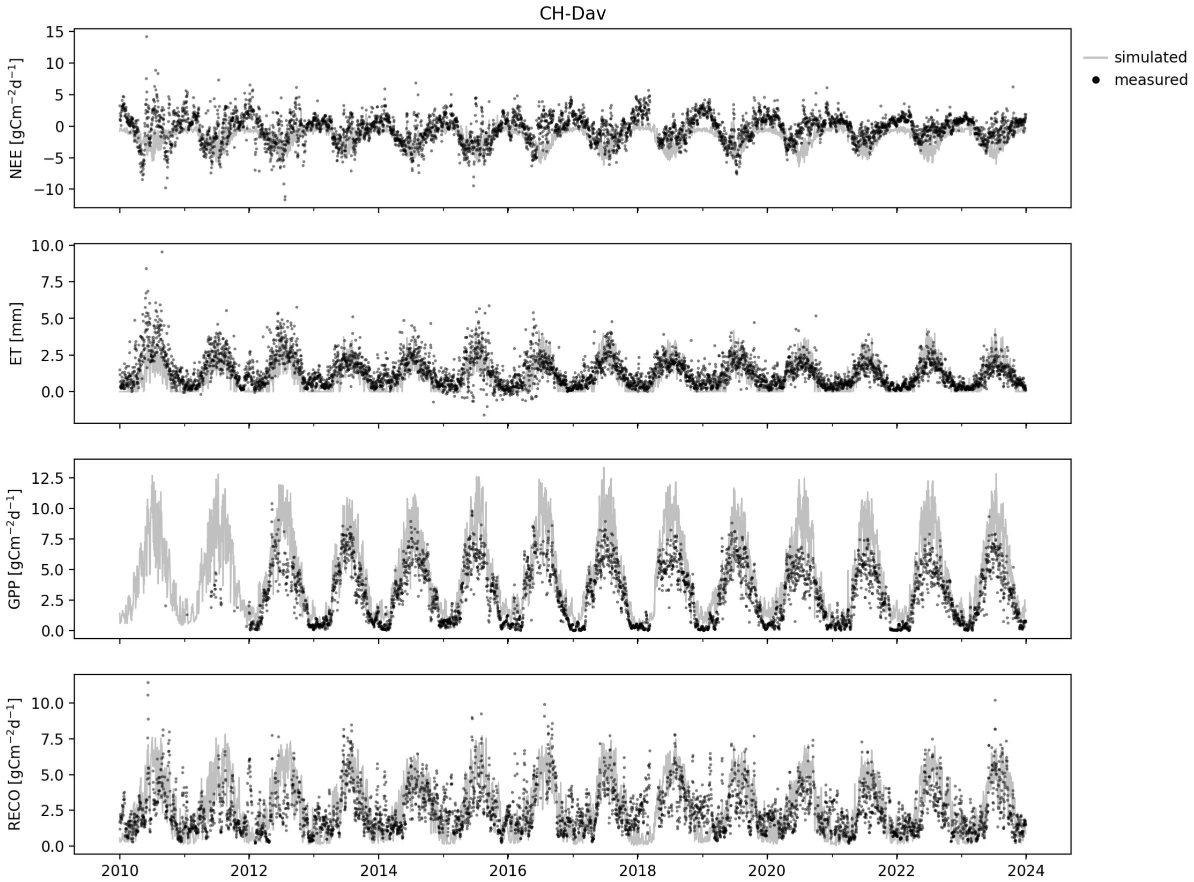

Fig. S4: Comparison of simulated (lines) and measured (dots) daily ecosystem fluxes at three spruce sites (top: BilyKriz, CZ, black dots; middle: Tharandt, DE, yellow dots; bottom: Davos, CH, green dots) throughout the years 2010-2023. NEE: net carbon exchange (gC m^{-2} d^{-1}), ET: evapotranspiration (mm), GPP: gross primary Productivity (gC m^{-2} d^{-1}), RECO: Ecosystem Respiration (gC m^{-2} d^{-1}).

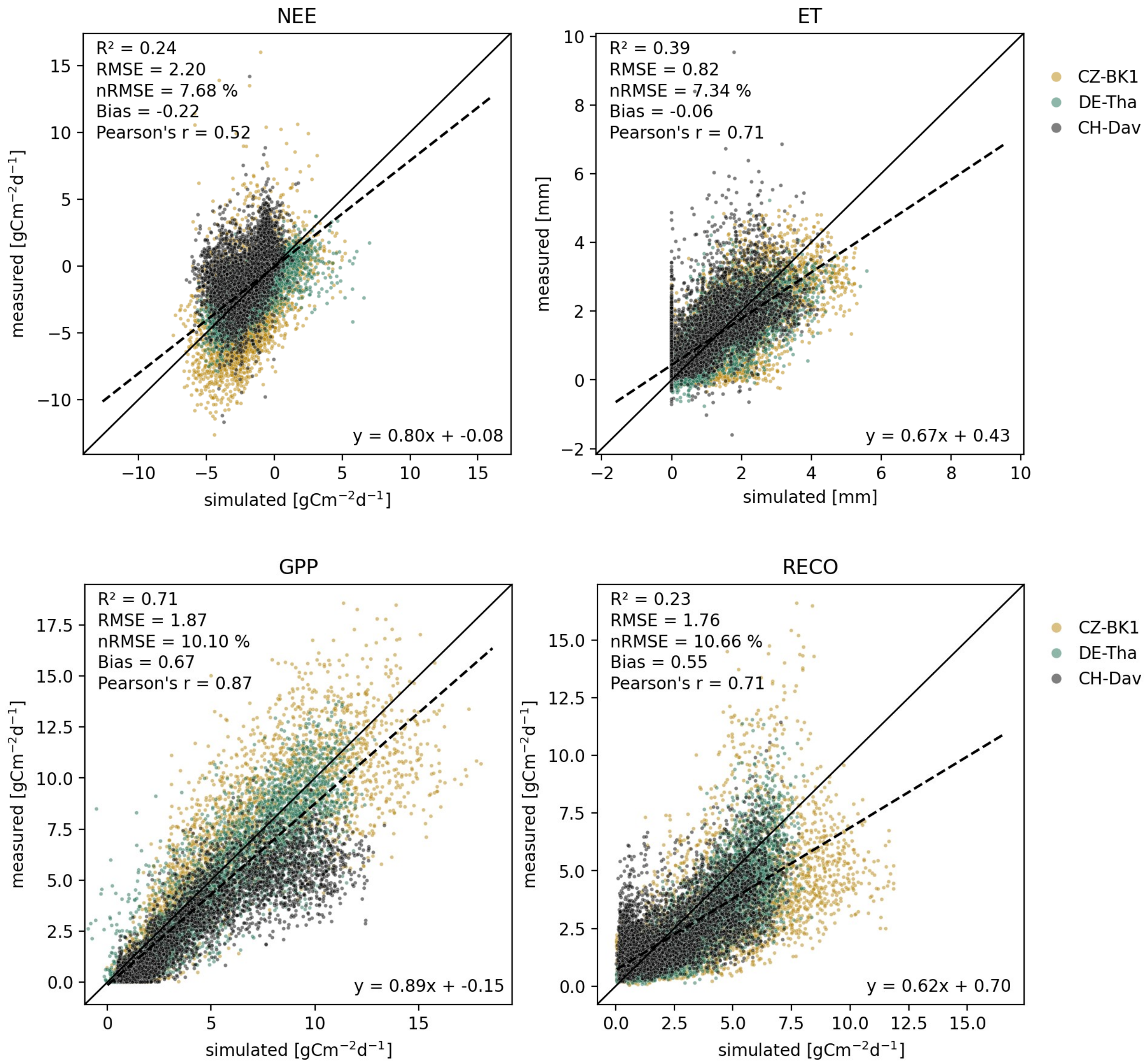

Fig. S5: Evaluation of simulated with measured daily ecosystem fluxes for all three spruce sites (see Fig. S3) for the whole available period. NEE (top-left): net ecosystem carbon exchange (gC m^{-2} d^{-1}), ET (top-right): evapotranspiration (mm), GPP (bottom-left): gross primary Productivity (gC m^{-2} d^{-1}), RECO (bottom-right): Ecosystem Respiration (gC m^{-2} d^{-1}). Different sites are depicted in different colors with the same color code as in Figures S1. Metrics include squared coefficient of determination (R^2), relative squared mean error (RSME), normalized relative squared mean error (nRSME), model bias (gC m $^{-2}$ d^{-1} and mm, respectively), and Pearson's coefficient of determination (r).

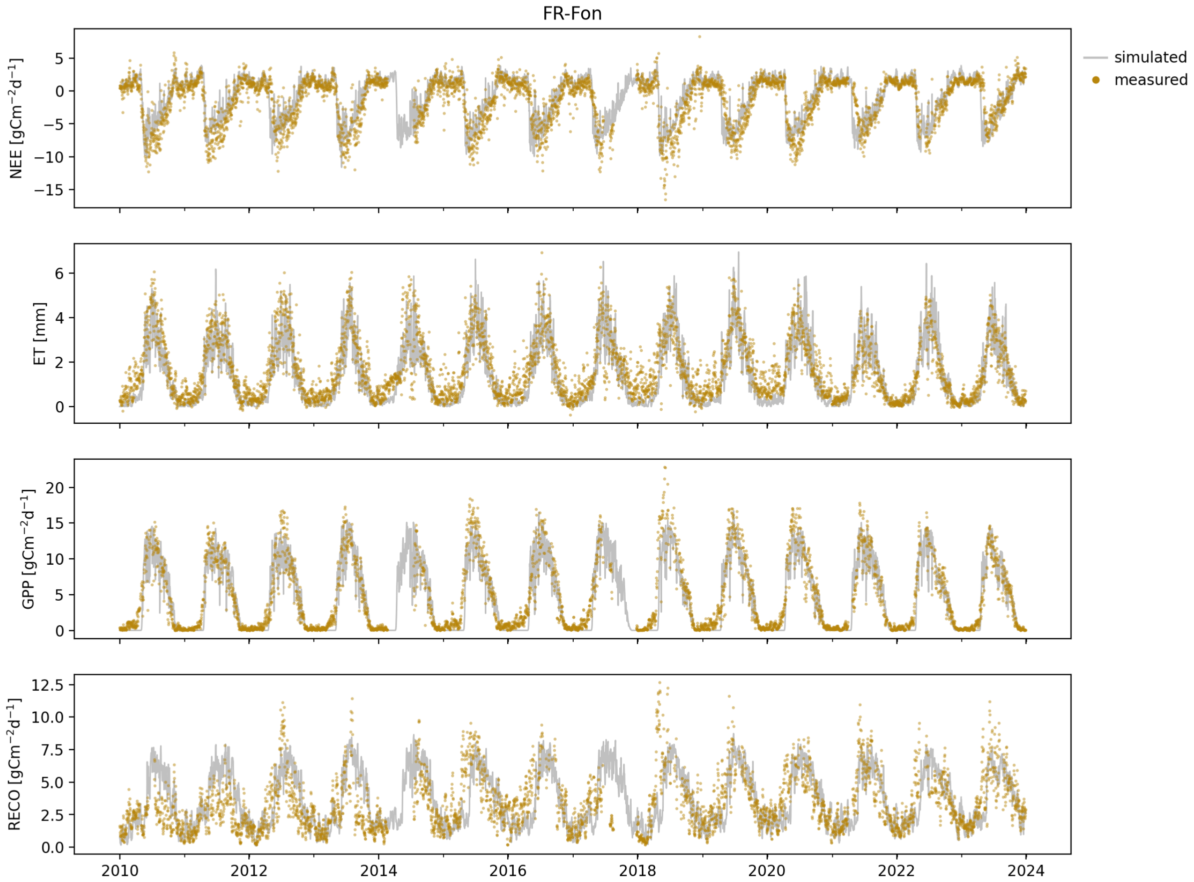
FR-Fon
simulated
measured
NEE [gCm⁻²d⁻¹]
ET [mm]
GPP [gCm⁻²d⁻¹]
RECO [gCm⁻²d⁻¹]
2010
2012
2014
2016
2018
2020
2022
2024

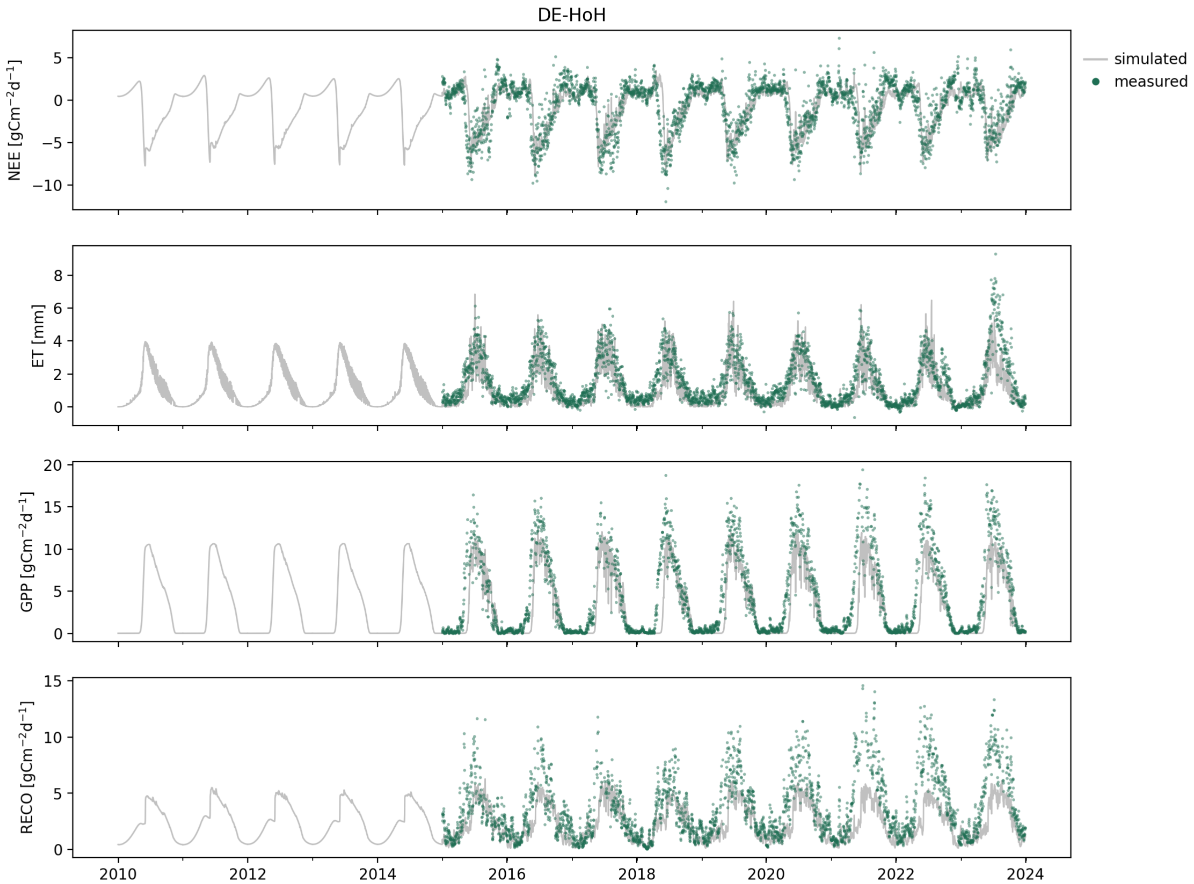
DE-HoH
simulated
measured
NEE [gCm⁻²d⁻¹]
ET [mm]
GPP [gCm⁻²d⁻¹]
RECO [gCm⁻²d⁻¹]
2010
2012
2014
2016
2018
2020
2022
2024

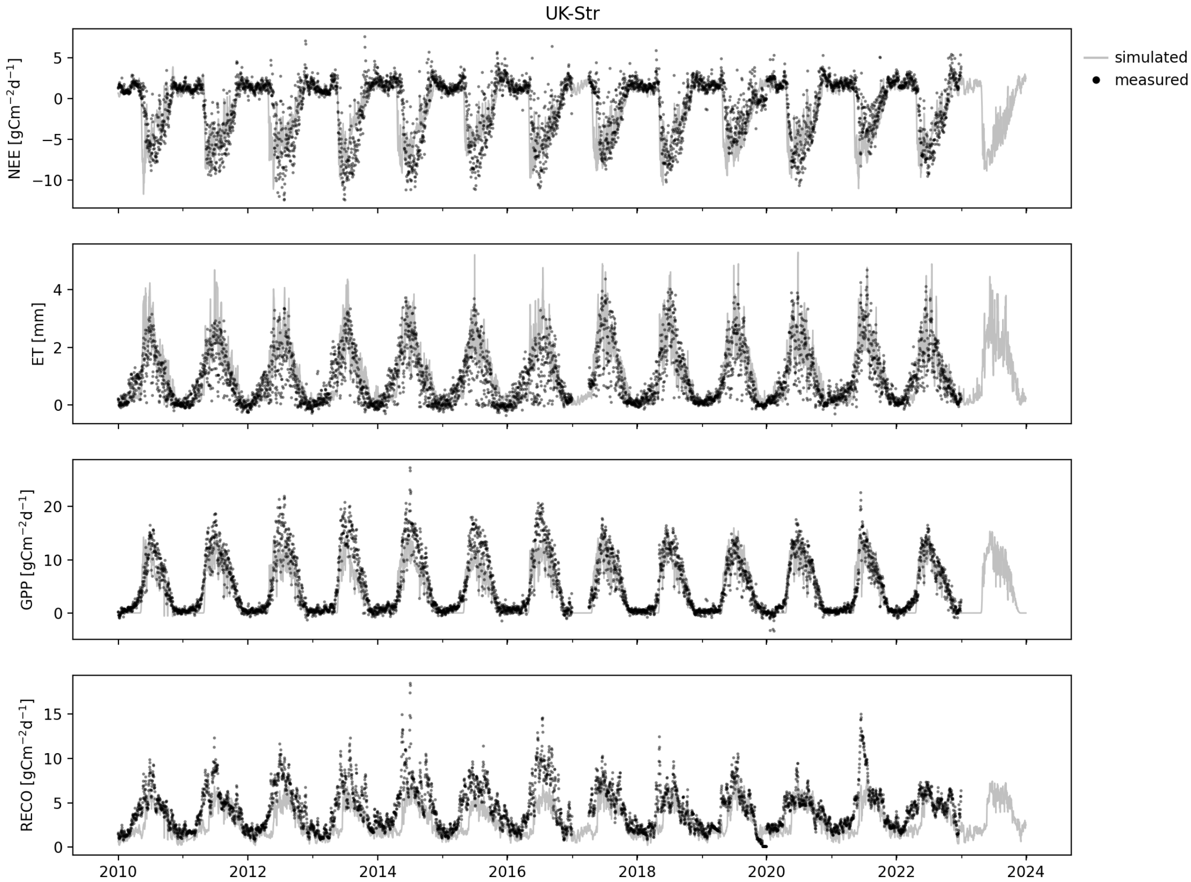

Fig. S6: Comparison of simulated (lines) and measured (dots) daily ecosystem fluxes at three oak sites (top: Fontainbleau, FR, black dots; middle: Hohes Holz, DE, yellow dots; bottom: Straits, UK, green dots) throughout the years 2010-2023. NEE: net carbon exchange (gC m^{-2} d^{-1}), ET: evapotranspiration (mm), GPP: gross primary Productivity (gC m^{-2} d^{-1}), RECO: Ecosystem Respiration (gC m^{-2} d^{-1}).

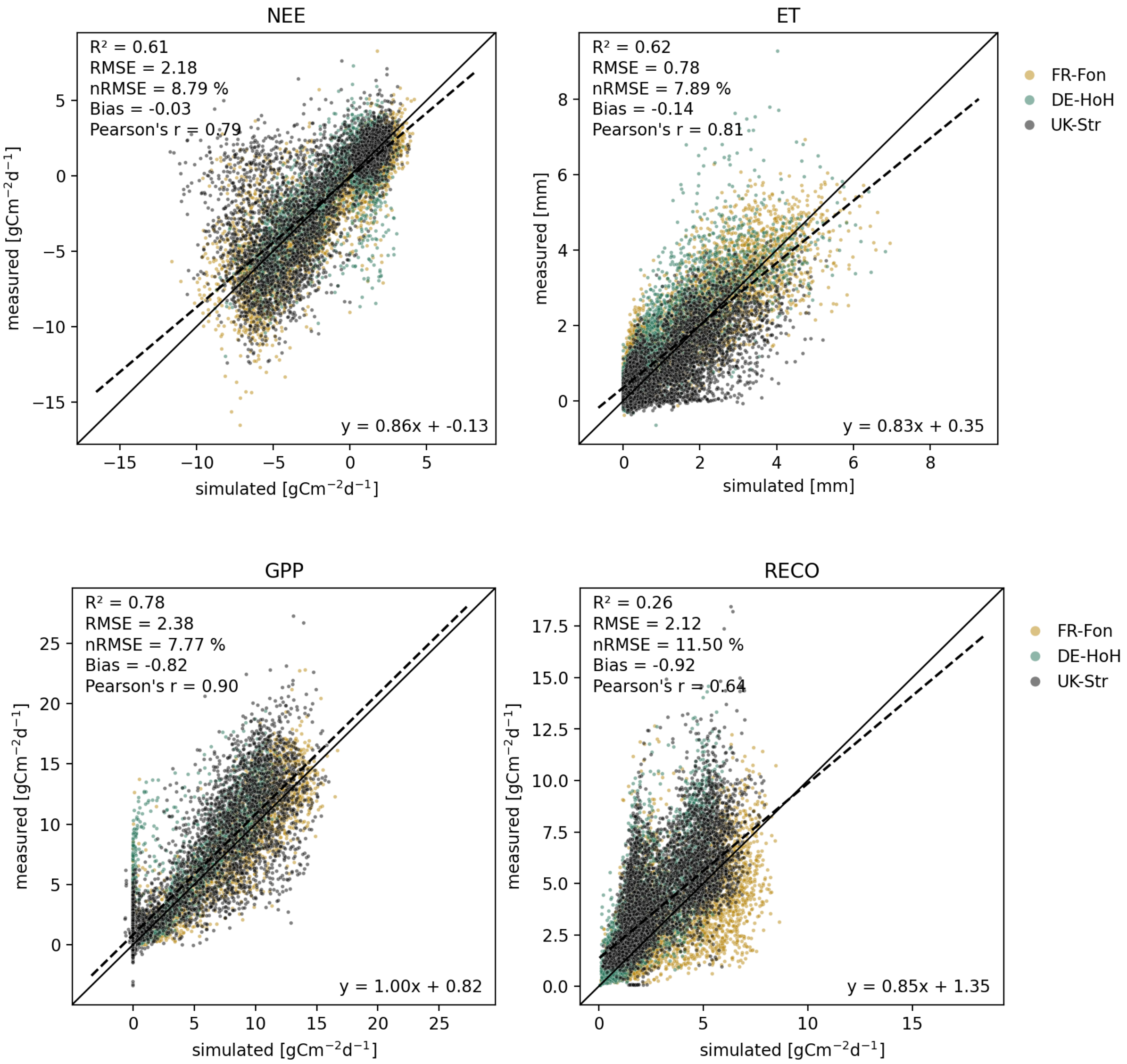

Fig. S7: Evaluation of simulated with measured daily ecosystem fluxes for all three oak sites (see Fig. S5) for the whole available period. NEE (top-left): net ecosystem carbon exchange (gC m^{-2} d^{-1}), ET (top-right): evapotranspiration (mm), GPP (bottom-left): gross primary Productivity (gC m^{-2} d^{-1}), RECO (bottom-right): Ecosystem Respiration (gC m^{-2} d^{-1}). Different sites are depicted in different colors with the same color code as in Figures S1. Metrics include squared coefficient of determination (R^2), relative squared mean error (RSME), normalized relative squared mean error (nRSME), model bias (gC m^{-2} d^{-1} and mm, respectively), and Pearson's coefficient of determination (r).

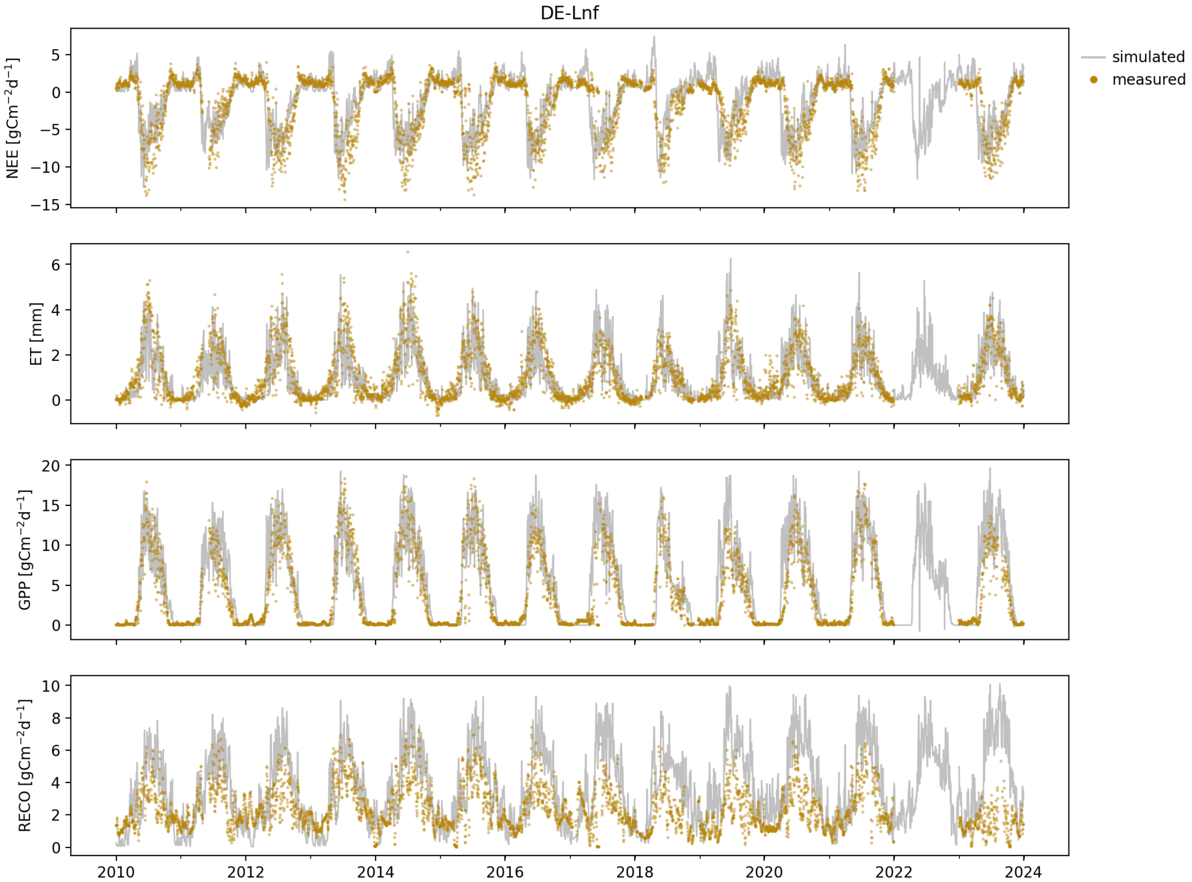
DE-Lnf
NEE [gCm⁻²d⁻¹]
ET [mm]
GPP [gCm⁻²d⁻¹]
RECO [gCm⁻²d⁻¹]
simulated
measured
2010
2012
2014
2016
2018
2020
2022
2024

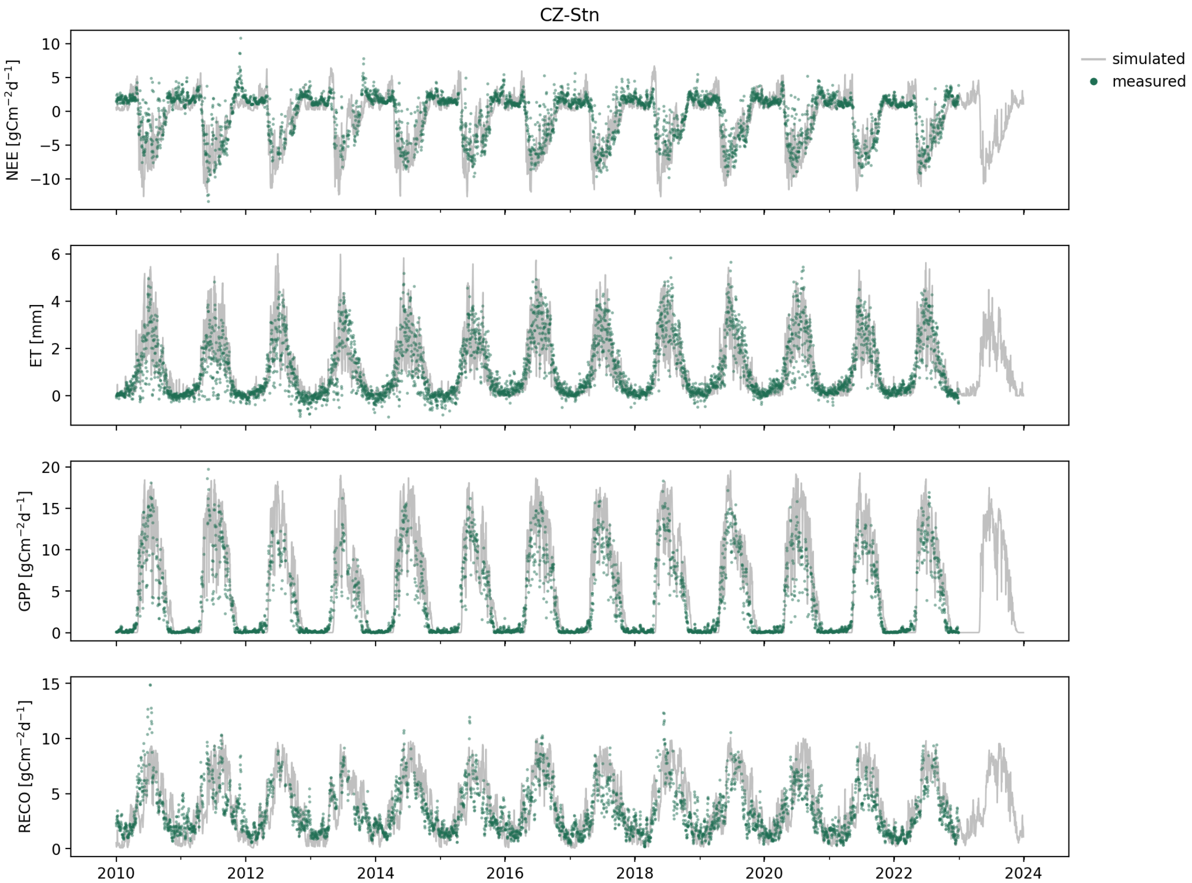
CZ-Stn
NEE [gCm⁻²d⁻¹]
ET [mm]
GPP [gCm⁻²d⁻¹]
RECO [gCm⁻²d⁻¹]
simulated
measured
2010
2012
2014
2016
2018
2020
2022
2024

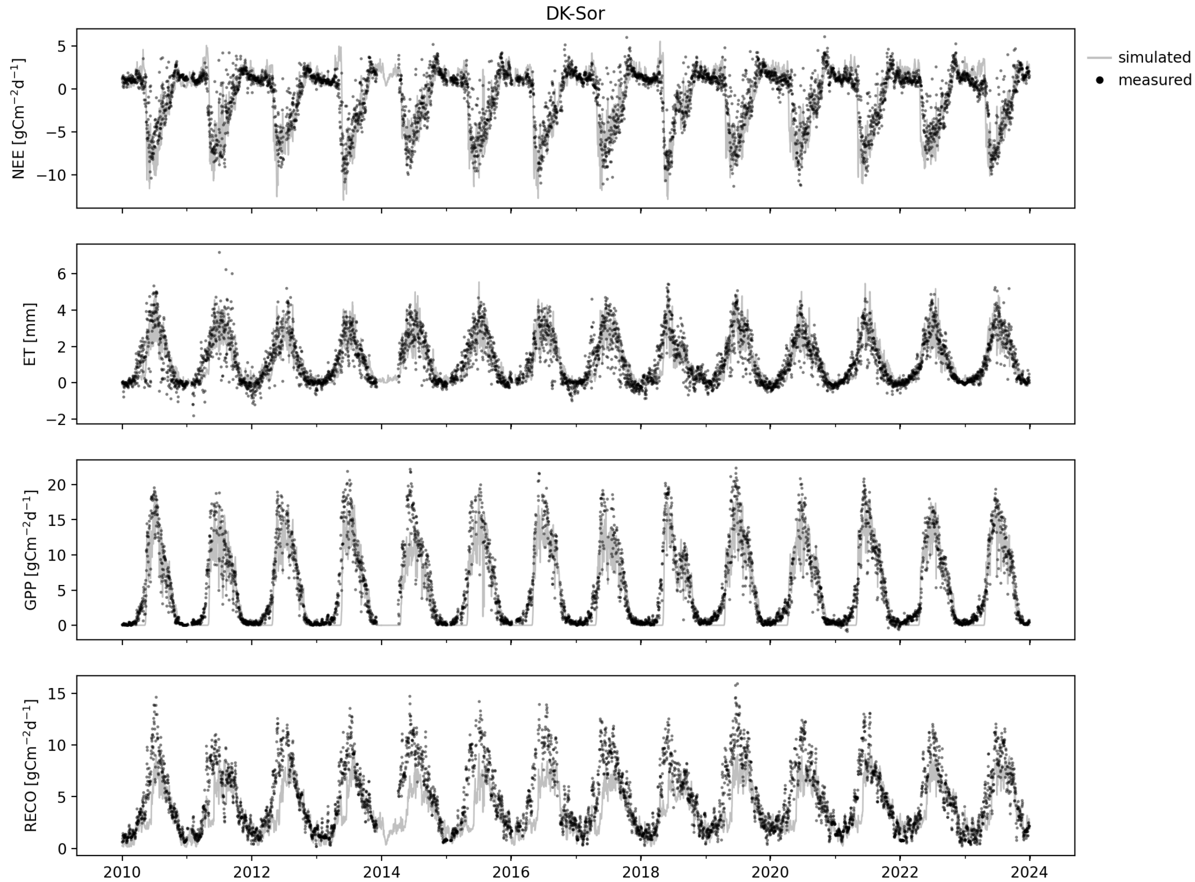

Fig. S8: Comparison of simulated (lines) and measured (dots) daily ecosystem fluxes at three beech sites (top: Soroe, DK, black dots; middle: Leinefelde, DE, yellow dots; bottom: Stitna, CZ, green dots) throughout the years 2010-2023. NEE: net carbon exchange (gC m^{-2} d^{-1}), ET: evapotranspiration (mm), GPP: gross primary Productivity (gC m^{-2} d^{-1}), RECO: Ecosystem Respiration (gC m^{-2} d^{-1}). Adapted from Moutahir et al., (2026).

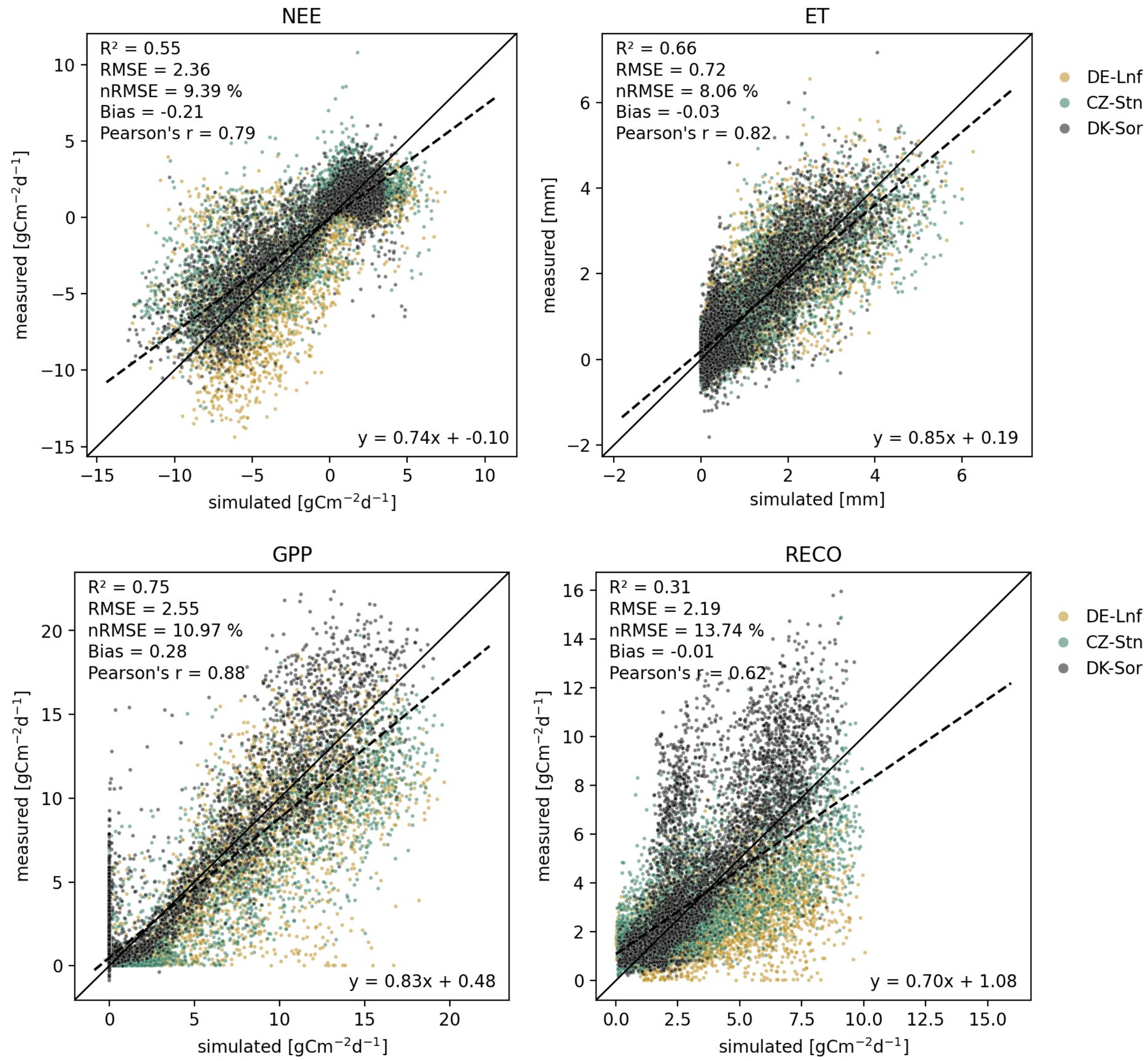

Fig. S9: Evaluation of simulated with measured daily ecosystem fluxes for all three beech sites (see Fig. S7) for the whole available period. NEE (top-left): net ecosystem carbon exchange (gC m^{-2} d^{-1}), ET (top-right): evapotranspiration (mm), GPP (bottom-left): gross primary Productivity (gC m^{-2} d^{-1}), RECO (bottom-right): Ecosystem Respiration (gC m^{-2} d^{-1}). Different sites are depicted in different colors with the same color code as in Figures S1. Metrics include squared coefficient of determination (R^2), relative squared mean error (RSME), normalized relative squared mean error (nRSME), model bias (gC m^{-2} d^{-1} and mm, respectively), and Pearson's coefficient of determination (r). Adapted from Moutahir et al., (2026) published under the Creative Commons Attribution 4.0 License (https://doi.org/10.5194/bg-23-1719-2026).

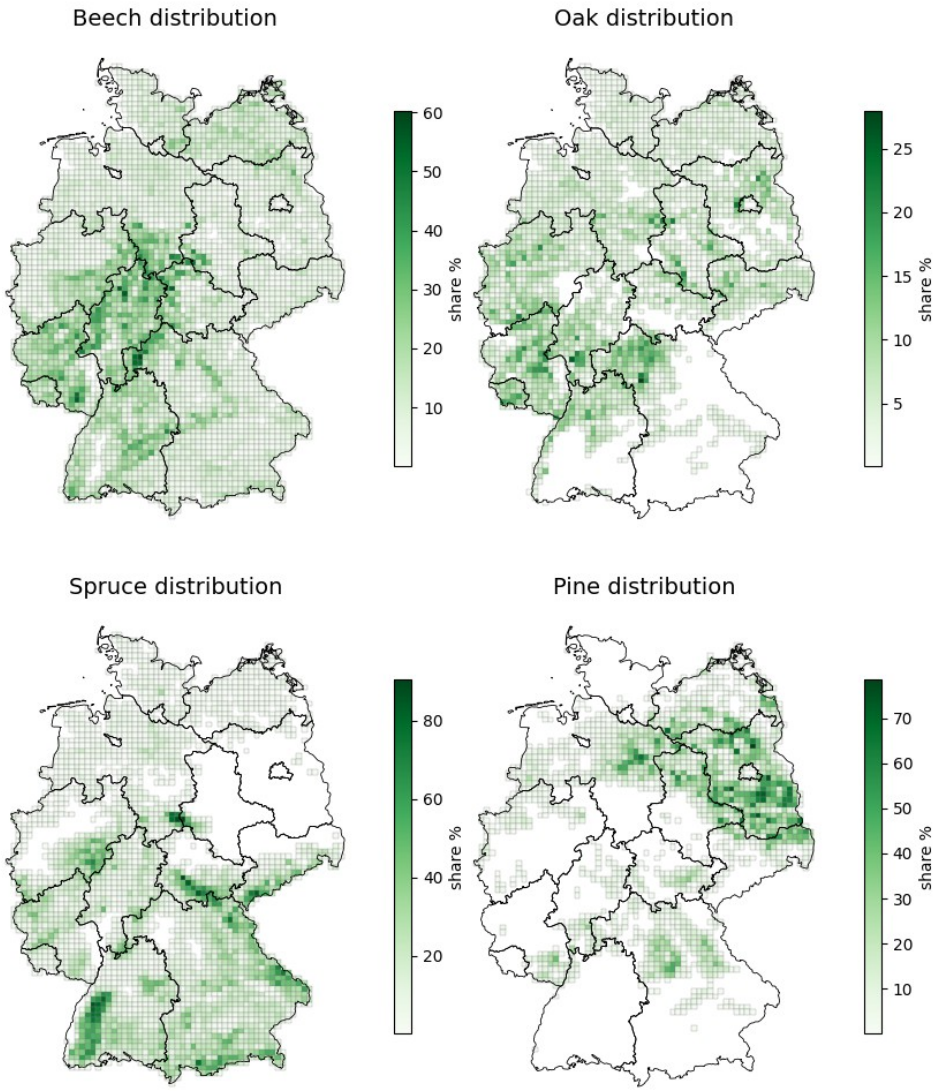

Fig. S10. Simulated 10×10 km gridcells with species-specific forest cover heatmaps for beech, oak, spruce, and pine with color intensity reflecting the local share of total forest area within each gridcell.

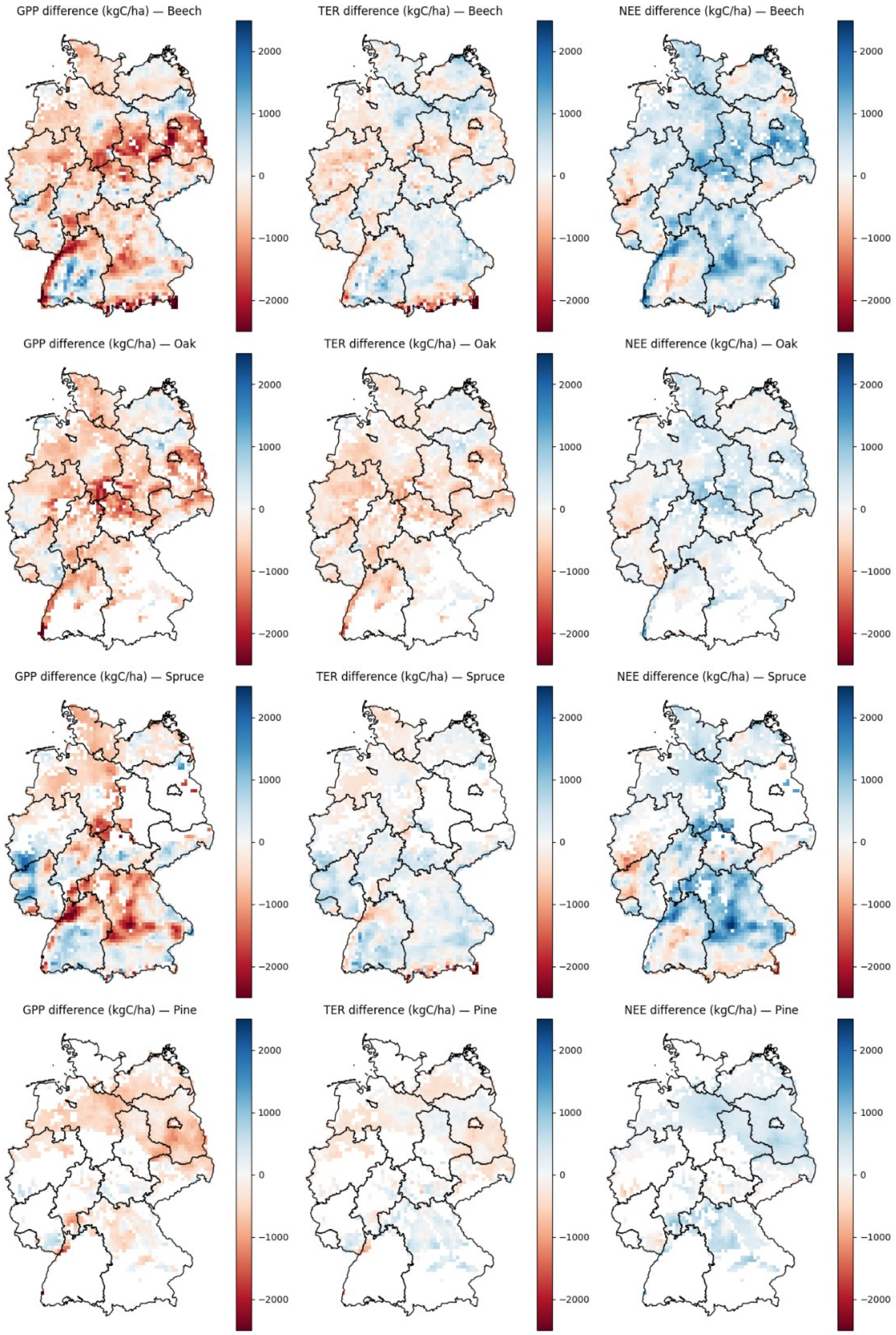

Fig. S11: Absolute differences (kg C ha^{-1}) in GPP, TER, and NEE (ERA5-Land minus E-OBS) forthe four tree species over the period 2011–2023. NEE is expressed as negative for carbon uptake; thus, positive values in the difference map correspond to reduced carbon uptake (weakened sink strength).

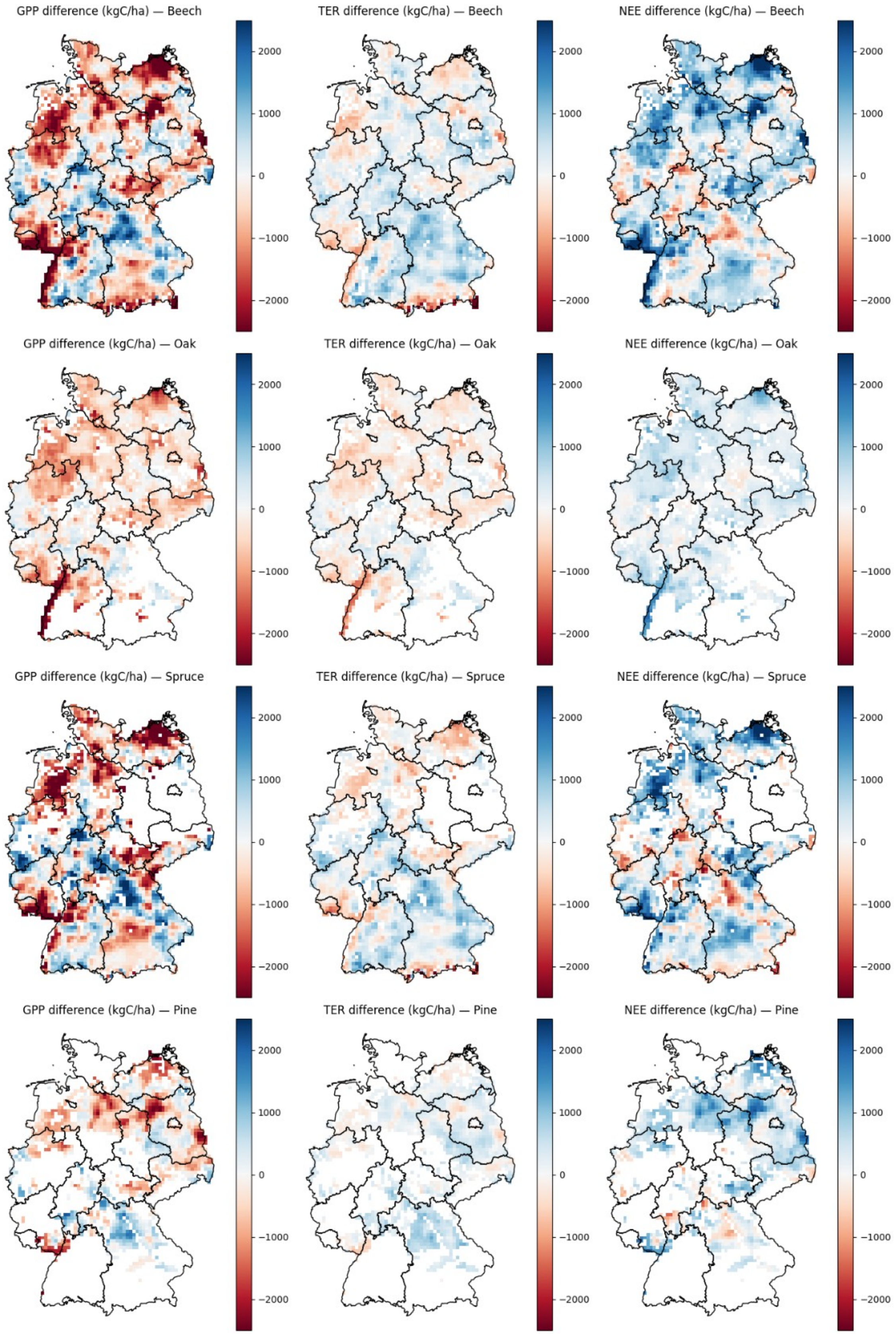

Fig. S12: Absolute differences (kg C ha⁻¹) in GPP, TER, and NEE (ERA5-Land minus E-OBS) forthe four tree species for the drought year 2018. NEE is expressed as negative for carbon uptake; thus, positive values in the difference map correspond to reduced carbon uptake (weakened sink strength).

Table S1: Characteristics of the twelve eddy-covariance forest sites used for model parameterization and evaluation.

Site name	Shortcut	Lat/Lon	Elevat-ion (m)	Species	Height (m)	N trees/ha	Air temperature (°C)	Precipitation (mm)	Humus type	Soil type	Rooting Depth (cm)
Brasschaat	BE-Bra	51.3076; 4.5198	16	Pinus sylvestris	21.3	384	11.1	815	Rawhumus	Loamy sand	112
Hyytiälä	FI-Hyy	61.8474; 24.2948	181	Pinus sylvestris	34.7	611	4.9	742	Moder	Sandy loam	70
Loobos	NL-Loo	52.1665; 5.7435	25	Pinus sylvestris	15.9	434	10.1	788	Moder	Sand	80
Tharandt	DE-Tha	50.9626; 13.5652	380	Picea abies	25.4	468	9.7	792	Moder	Silt loam	122
Davos	CH-Dav	46.8153; 9.8559	1639	Picea abies	25	1100	4.6	858	Rawhumus	Sandy loam	90
Bílý Kříž	CZ-BK1	49.5021; 18.5369	875	Picea abies	11	1430	6.9	1140	Moder	Sandy loam	45
Hohes Holz	DE-HoH	52.0865; 11.2223	193	Oak-dominated deciduous	29.6	100	10.2	485	Mull	Silt loam	183
Fontainebleau -Barbeau	FR-Fon	48.4763; 2.7801	103	Quercus petraea / Q. robur	25	280	11.9	650	Mull	Sandy clay	300
Straits	UK-Str	51.1167; -0.8500	80	Oak plantation	21.1	345	10.7	782	Mull	Silty clay	102
Leinefelde	DE-Lnf	51.3282; 10.3678	450	Fagus sylvatica	34	224	8	620	Mull	Silty clay	103
Sorø	DK-Sor	55.4869; 11.6458	40	Fagus sylvatica	25.5	420	9	850	Mull	Sandy loam	113
Stitná	CZ-Stn	49.0359; 17.9699	562	Fagus sylvatica	30.5	286	9.1	655	Mull	Silt loam	125

Table S2: Parameters affecting the simulation of carbon and water exchange in the LandscapeDNDC model. Values are mostly taken from the literature but '*' indicate that they are calibrated within boundaries reported in the literature using specific sites (see Fig. S1 to 8).

Variable	Description	Beech	Oak	Spruce	Pine	References (Beech; Oak; Spruce; Pine)
Photosynthesis						
AEKC	Activation energy for Michaelis-Menten constant for CO_2 (J mol^{-1})	80500	65000	65000	59400	Harley & Baldocchi (1995); Werner et al. (2001); Falge et al. (1997); Medlyn et al. (2002)
AEKO	Activation energy for Michaelis-Menten constant for O_2 (J mol^{-1})	14500	36000	36000	36000	Harley & Baldocchi (1995); Werner et al. (2001); Falge et al. (1997); Medlyn et al. (2002)
AERD	Activation energy for dark respiration (J mol^{-1})	36500	41550	63500	42580	Dreyer et al. (2001); Dreyer et al. (2001); Falge et al. (1997); Wang et al. (1996)
AEVC	Activation energy for photosynthesis (J mol^{-1})	70627	55729	75750	69830	Kattge & Knorr (2007); Kattge & Knorr (2007); Falge et al. (1997); Wang et al. (1996)
AEVO	Activation energy for RubP oxygenation (J mol^{-1})	37530	37530	37530	37530	Long (1991) (all species)
AEJM	Activation energy for electron transport (J mol^{-1})	48090	40719	40000	61650	Medlyn et al. (2002); Kattge & Knorr (2007); Ibrom et al. (2006); Wang et al. (1996)
KC25	Michaelis-Menten constant for CO_2	275	275	460	405	Harley & Baldocchi (1995); Harley & Baldocchi (1995); Farquhar et al. (1980); Medlyn et al. (2002)
KO25	Michaelis-Menten constant for O_2	420	420	330	278.4	Harley & Baldocchi (1995); Harley & Baldocchi (1995); Farquhar et al. (1980); Medlyn et al. (2002)
QVOVC	Relation between saturated rate of oxygenation and carboxylation	0.21	0.21	0.21	0.21	Long (1991) (all species)
QJVC	Relation between max. electron transport rate and RubP-saturated carboxylation	2.24	1.83	2.47	2.48	Yan et al. (2023); Kattge & Knorr (2007); Grassi et al. (2001); Samson et al. 2006
QRD25	Relation between dark respiration rate and carboxylation capacity	0.0149	0.024	0.022	0.003	Yan et al. (2023); Dreyer et al. (2001); Ibrom et al. (2006); Wang et al. 1996
SLOPE_GSA	Slope of stomata response in the BERRY-BALL model	11.8	3.94	6.4	5	Medlyn et al. (2001); Medlyn & Jarvis (1999); Medlyn et al. (2001); Kellomäki & Wang (1996)
THETA	Curvature parameter for photosynthesis	0.882	0.85	0.71	0.7	Yan et al. (2023); Werner et al. (2001); Medlyn et al. (2005); Aalto et al. (2002)
VCMAX25	Saturated rate of carboxylation at 25 oC (µmol m^{-2} s^{-1})	38	60	120	95	*
Water exchange						
GSmax	Maximum stomata conductivity (mmol H2O m^{-2} s^{-1})	497.3	350	48	600	*
GSmin	Minimum stomata conductivity (mmol H2O	9.1	20	1.5	15	*

	m⁻² s⁻¹)					
H2OREF_GS	Relative available soil water content at which stomata closure starts	0.3	0.4	0.23	0.15	*
WUECmax	Maximum water use efficiency (mg H2O g C^{-1})	23.7	25	20	18	*
WUECmin	Minimum water use efficiency (mg H2O g C^{-1})	4	2	10	10	*
Phenology						
DLEAFSHED	Total leaf longevity from emergence (days)	350	330	3030	1409	*
GDDFOLSTART	Temperature sum for foliage activity onset (°C)	282	100	236	110	*
MFOLopt	Foliage biomass for mature stands under closed canopy condition (kg m^{-2})	0.25	0.43	1.3	0.45	*
NDFLUSH	Time interval necessary to complete flushing of foliage (days)	21	60	62	67	*
NDMORT	Time interval necessary to complete litterfall (days)	106	60	376	165	*
SLAmax	Specific leaf area in the shade (m^2 kg^{-1})	31	20	6.8	9.1	Aranda et al. (2004); Cermak (1998); Perterer & Körner (1990); Moren et al. (2000)
SLAmin	Specific leaf area in full light (m^2 kg^{-1})	11	5.9	2.1	3.4	Aranda et al. (2004); Cermak (1998); Perterer & Körner (1990); Moren et al. (2000)
Others						
ALB	Foliage albedo	0.05	0.18	0.06	0.11	Dufrene et al. (2005); Otto et al. (2005); Jarvis et al. (1976); Perttu et al. (1980)
EXT	Light extinction factor	0.53	0.54	0.42	0.56	Molina-Herrera et al. (2015); Li et al. (1997); Forrester et al. (2014); Molina-Herrera et al. (2015)
KM20	Maintenance coefficient at reference temperature of 20 oC	0.9	0.45	0.5	1.5	*
NCFOLopt	Optimum nitrogen concentration of foliage (%)	0.03	0.03	0.02	0.01	Mellert & Göttlein (2012); Mellert & Göttlein (2012); Mellert & Göttlein (2012); Molina-Herrera et al. (2015)

Table S3: Number of simulated grid cells and sampling points per tree group

Tree group	Total grid cells with tree group	Excluded grid cells	% of excluded tree group area	Simulated grid cells	Sampling points
Beech	3655	66	0.36	3589	53835
Oak	3639	1010	5.14	2629	39435
Spruce	3638	929	0.99	2709	40635
Pine	3524	2060	2.47	1464	21960

Table S4. Mean (± standard deviation) difference of climate variables over Germany (2011–2023) between ERA5-Land and E-OBS

Variable	ERA5	E-OBS	ERA5 − E-OBS	(ERA5 − E-OBS) / E-OBS (%)
Precipitation (mm yr⁻¹)	872.1 ± 202.8	740.5 ± 212.7	132.5 ± 88.4	19.8 ± 11.9
Mean temperature (°C)	9.9 ± 0.9	9.8 ± 0.9	0.1 ± 0.4	1.0 ± 5.0
Maximum temperature (°C)	13.5 ± 0.9	14.4 ± 1.0	−0.8 ± 0.4	−5.7 ± 3.2
Minimum temperature (°C)	6.2 ± 1.1	5.3 ± 0.9	0.9 ± 0.7	17.4 ± 12.1
Diurnal temperature range (°C)	7.3 ± 0.8	9.1 ± 0.8	−1.7 ± 0.7	−18.6 ± 7.0
Global radiation (W m⁻²)	130.2 ± 7.2	126.0 ± 6.16	4.2 ± 1.0	3.3 ± 1.8

References :

Aalto, T., Hari, P., & Vesala, T. (2002). Comparison of an optimal stomatal regulation model and a biochemical model in explaining CO2 exchange in field conditions. Silva Fennica, 36(3), 615–623.

Aranda, I., Pardo, F., Gil, L., & Pardos, J. A. (2004). Anatomical basis of the change in leaf mass per area and nitrogen investment with relative irradiance within the canopy of eight temperate tree species. Acta Oecologica, 25, 187–195.

Bequet, R., Kint, V., Campioli, M., Vansteenkiste, D., Muys, B., & Ceulemans, R. (2012). Influence of stand, site and meteorological variables on the maximum leaf area index of beech, oak and Scots pine. European Journal of Forest Research, 131(2), 283–295.

Carrara, A., Kowalski, A. S., Neirynck, J., Janssens, I. A., Curiel Yuste, J., & Ceulemans, R. (2003). Net ecosystem CO2 exchange of mixed forest in Belgium over 5 years. Agricultural and Forest Meteorology, 119, 209–227.

Cermak, J. (1998). Leaf distribution in large trees and stands of the floodplain forest in southern Moravia. Tree Physiology, 18, 727–737. https://doi.org/10.1093/treephys/18.11.727

Delpierre, N., Berveiller, D., Granda, E., & Dufrêne, E. (2016). Wood phenology, not carbon input, controls the interannual variability of wood growth in a temperate oak forest. New Phytologist, 210(2), 459–470. https://doi.org/10.1111/nph.13771

Dreyer, E., Le Roux, X., Montpied, P., Daudet, F. A., & Masson, F. (2001). Temperature response of leaf photosynthetic capacity in seedlings from seven temperate tree species. Tree Physiology, 21, 223–232. https://doi.org/ 10.1093/treephys/21.4.223

Dufrene, E., Davi, H., Francois, C., Le Maire, G., Le Dantec, V., & Granier, A. (2005). Modelling carbon and water cycles in a beech forest Part I: Model description and uncertainty analysis on modelled NEE. Ecological Modelling, 185, 407–436. https://doi.org/10.1016/j.ecolmodel.2005.01.004

Etzold, S., Ruehr, N. K., Zweifel, R., Dobbertin, M., Zingg, A., Pluess, P., Häsler, R., Eugster, W., & Buchmann, N. (2011). The Carbon Balance of Two Contrasting Mountain Forest Ecosystems in Switzerland: Similar Annual Trends, but Seasonal Differences. Ecosystems, 14(8), 1289–1309. https://doi.org/10.1007/s10021-011-9481-3

Falge, E., Ryel, R. J., Alsheimer, M., & Tenhunen, J. D. (1997). Effects of stand structure and physiology on forest gas exchange: a simulation study for Norway spruce. Trees-Structure and Function, 11(7), 436–448.

Farquhar, G. D., Von Caemmerer, S., & Berry, J. A. (1980). A biochemical model of photosynthetic CO2 assimilation in leaves of C3 species. Planta, 149, 78–90. https://doi.org/10.1007/BF00386231

Forrester, D. I. (2014). A stand-level light interception model for horizontally and vertically heterogeneous canopies. Ecological Modelling, 276, 14–22. https://doi.org/10.1016/j.ecolmodel.2013.12.021

Grünwald, T., & Bernhofer, C. (2007). A decade of carbon, water and energy flux measurements of an old spruce forest at the Anchor Station Tharandt. Tellus Series B-Chemical and Physical Meteorology, 59(3), 387–396.

Harley, P. C., & Baldocchi, D. D. (1995). Scaling carbon dioxide and water vapour exchange from leaf to canopy in a deciduous forest. I. Leaf model parameterization. Plant, Cell & Environment, 18(10), 1146–1156. https://doi.org/10.1111/j.1365-3040.1995.tb00625.x

Ibrom, A., Jarvis, P. G., Clement, R., Morgenstern, K., Oltchev, A., Medlyn, B. E., Wang, Y. P., Wingate, L., Moncrieff, J. B., & Gravenhorst, G. (2006). A comparative analysis of simulated and observed photosynthetic CO2 uptake in two coniferous forest canopies. Tree Physiology, 26(7), 845–864.

Jarvis, P. G. (1976). The interpretation of leaf water potential and stomatal conductance found in canopies in the field. Philosophical Transactions of the Royal Society B: Biological Sciences, 273, 593–610. https://doi.org/10.1098/rstb.1976.0035

Kattge, J., & Knorr, W. (2007). Temperature acclimation in a biochemical model of photosynthesis: a reanalysis of data from 36 species. Plant, Cell & Environment, 30(9), 1176–1190. https://doi.org/10.1111/j.1365-3040.2007.01690.x

Lange, M., Dechant, B., Rebmann, C., Vohland, M., Cuntz, M., & Doktor, D. (2017). Validating MODIS and Sentinel-2 NDVI Products at a Temperate Deciduous Forest Site Using Two Independent Ground-Based Sensors. Sensors, 17(8), 1855. https://doi.org/10.3390/s17081855

Li, H., Wen, Z., Huang, M., & Wang, M. (1997). A genetic study on characteristics of crown light interception in Populus deltoides. Canadian Journal of Forest Research, 27(9), 1465–1470. https://doi.org/10.1139/x97-101

Long, S. P. (1991). Modification of the response of photosynthetic productivity to rising temperature by atmospheric CO2 concentrations: Has its importance been underestimated? Plant, Cell & Environment, 14(8), 729–739. https://doi.org/10.1111/j.1365-3040.1991.tb01439.x

Medlyn, B. E., Berbigier, P., Clement, R., Grelle, A., Loustau, D., Linder, S., Wingate, L., Jarvis, P. G., Sigurdsson, B. D., & McMurtrie, R. E. (2005). Carbon balance of coniferous forests growing in contrasting climates: Model-based analysis. Agricultural and Forest Meteorology, 131, 97–124. https://doi.org/10.1016/j.agrformet.2005.05.004

Medlyn, B. E., Dreyer, E., Ellsworth, D., Forstreuter, M., Harley, P. C., Kirschbaum, M. U. F., Le Roux, X., Montpied, P., Strassmeyer, J., Walcroft, A., Wang, K., & Loustau, D. (2002). Temperature response of parameters of a biochemically based model of photosynthesis. II. A review of experimental data. Plant, Cell & Environment, 25(9), 1167–1179. https://doi.org/10.1046/j.1365-3040.2002.00891.x

Mellert, K., & Göttlein, A. (2012). Comparison of new foliar nutrient thresholds derived from van den Burg's literature compilation with established central European references. European Journal of Forest Research, 131(5), 1461–1472.

Molina-Herrera, S., Grote, R., Santabárbara-Ruiz, I., Kraus, D., Klatt, S., Haas, E., Kiese, R., & Butterbach-Bahl, K. (2015). Simulation of CO2 fluxes at European forest ecosystems with the coupled soil-vegetation process model “LandscapeDNDC”. Forests, 6, 1779–1809. https://doi.org/10.3390/f6061779

Moren, A. S., Lindroth, A., & Grelle, A. (2001). Water-use efficiency as a means of modelling net assimilation in boreal forests. Trees-Structure and Function, 15(2), 67–74.

Moutahir H, Sulzer M, Kiese R, Christen A, Weiler M et al (2026) Matching scales of eddy covariance measurements and process-based modeling – assessing spatiotemporal dynamics of carbon and water fluxes in a mixed forest in Southern Germany. Biogeosciences 23:1719–1738. https://doi.org/10.5194/bg-23-1719-2026

Nadal-Sala, D., Grote, R., Birami, B., Lintunen, A., Mammarella, I., Preisler, Y., Rotenberg, E., Salmon, Y., Tatrinov, F., Yakir, D., & Ruehr, N. (2021). Assessing model performance via the most limiting environmental driver (MLED) in two differently stressed pine stands. Ecological Applications, 31(4), e02312. https://doi.org/10.1002/eap.2312

Otto, J., Berveiller, D., Bréon, F. M., Delpierre, N., Geppert, G., Granier, A., Jans, W., Knohl, A., Kuusk, A., Longdoz, B., Moors, E., Mund, M., Pinty, B., Schelhaas, M. J., & Luyssaert, S. (2014). Forest summer albedo is sensitive to species and thinning: how should we account for this in Earth system models? Biogeosciences, 11(8), 2411–2427. https://doi.org/10.5194/bg-11-2411-2014

Perterer, J., & Körner, C. (1990). Das Problem der Bezugsgröße bei physiologisch-ökologischen Untersuchungen an Koniferennadeln. Forstwissenschaftliches Centralblatt, 109, 220–241.

Perttu, K., Bischof, W., Grip, H., Jansson, P.-E., Lindgren, A., Lindroth, A., & Norén, B. (1980). Micrometeorology and hydrology of pine forest ecosystems. I. Field studies. In T. Persson (Ed.), Structure and function of northern Coniferous forests - An ecosystem Study (Vol. 32, pp. 75–121).

Sedlák, P., Aubinet, M., Heinesch, B., Janouš, D., Pavelka, M., Potužníková, K., & Yernaux, M. (2010). Night-time airflow in a forest canopy near a mountain crest. Agricultural and Forest Meteorology, 150(5), 736–744. https://doi.org/https://doi.org/10.1016/j.agrformet.2010.01.014

Van Genuchten, M. T. (1980). A closed-form equation for predicting the hydraulic conductivity of unsaturated soils. Soil Science Society of America Journal, 44, 892–898. https://doi.org/10.2136/sssaj1980.03615995004400050002x

Vesala, T., Haataja, J., Aalto, P. P., Altimir, N., Buzorius, G., Hämeri, K., Ilvesniemi, H., Jokinen, V., Keronen, P., Lahti, T., Markkanen, T., Mäkelä, J. M., Nikinmaa, E., Palmroth, S., Pohja, T., Pumpanen, J., Rannik, U. l., Siivola, E., Ylitalo, H.,…Kulmala, M. (1998). Long-term field measurements of atmosphere-surface interactions in boreal forest combining forest ecology, micrometeorology, aerosol physics and atmospheric chemistry. Trends in Heat, Mass & Momentum Transfer, 4, 17–35.

Wang, K.-Y., Kellomäki, S., & Laitinen, K. (1996). Acclimation of photosynthetic parameters in Scots pine after three years of exposure to elevated temperature and CO2. Agricultural and Forest Meteorology, 82, 195–217.

Werner, C., Ryel, R. J., Correia, O., & Beyschlag, W. (2001). Effects of photoinhibition on whole-plant carbon gain assessed with a photosynthesis model. Plant, Cell & Environment, 24(1), 27–40. https://doi.org/10.1046/j.1365-3040.2001.00651.x

Wilkinson, M., Eaton, E. L., Broadmeadow, M. S. J., & Morison, J. I. L. (2012). Inter-annual variation of carbon uptake by a plantation oak woodland in south-eastern England. Biogeosciences, 9(12), 5373–5389. https://doi.org/10.5194/bg-9-5373-2012

Yan, Y., Klosterhalfen, A., Moyano, F., Cuntz, M., Manning, A. C., & Knohl, A. (2023). A modeling approach to investigate drivers, variability and uncertainties in O2 fluxes and O2 : CO2 exchange ratios in a temperate forest. Biogeosciences, 20(19), 4087–4107. https://doi.org/10.5194/bg-20-4087-2023